

# High-efficiency Operation of Switched Reluctance Generator based on Current Waveform Control

Zhenguo Li \*, Siyang Yu \*\* and Jin-Woo Ahn \*\*

**Abstract** –The main aim of this paper is to expound high-efficiency operation of Switched Reluctance Generator (SRG) based on the current waveform. For this purpose, theoretical analysis of the copper loss and iron loss of the system is done first. Then, necessary simulation is done to find the variation trend of the copper loss and iron loss with the variation of the current waveform at the same output power. Finally, the best current waveform which can make the system operate with high efficiency is obtained by considering the influence of these two kinds of loss. In order to verify the simulation results, the experimental platform of DC motor-SRG is built and the modified angle position control (APC) method which can specify the current shape optionally is presented. By comparing the system efficiency at the three kinds of typical current waveform, the correctness and feasibility of the theory is verified. The proposed method is simple, reliable, and easy to achieve.

**Keywords:** Switched Reluctance Generator, Current Waveform Control, Power Closed-Loop Control, High-Efficiency Operation

## 1. Introduction

There are so many advantages of the SRG, such as simple construction, low manufacturing cost, low inertia, fault tolerance and the ability to operate in a high temperature environment [1]. The SRG is under development for drives in power source applications that include hybrid electric vehicles, aerospace power systems and wind engines [2~3]. The aerospace and automotive applications are characterized by high-speed operation and constant mechanical power is provided over a wide speed range, while the wind energy applications are characterized by low-speed and high-torque operation. The objective of SRG control is normally to track the output power and keep the DC-link voltage at a desired value with high-efficiency, low-torque ripple, and low-acoustic noise. These control objectives can be optimized by appropriately adjusting the turn-on/off angles and other parameters of the SRG.

At present, the relevant literature about improving the system efficiency of SRG is little. In [4], the control of excitation of SRG for maximum efficiency at single pulse mode of operation has been presented. Turn on and turn off

angles are defined as control variables, turn on angle is set based on the output power and the turn off angle is selected to achieve optimal efficiency at each power level and speed. In [5], a loss minimization method for an SRM with speed control has been presented. The duty cycle of the applied DC voltage for achieving the required speed is controlled with an inner loop controller. When the motor is stationary, the turn on angle is chosen such that the energy losses are minimized. Current chopping control and single pulse control are adopted respectively as inner loop to hold-on DC-link voltage in [6] and [7]. Moreover, optimal turn-on/turn-off angles can be chosen by analysis of the system efficiency and torque ripple in [6] while, in [7] by a ratio of two fluxes, the flux where entire-overlapped stator and rotor poles start to detach and the max flux linkage. Based on measured magnetization curve, optimal on/off angle can be obtained by analysis of output power and system efficiency under a series of different on/off angles in [8].

This paper mainly analyzes the effect of phase current waveform on the power closed-loop system efficiency during the SRG system power generation stage. The best current waveform which can make the system operate with high efficiency is obtained by theoretical analysis and simulation of the copper loss and core loss. The correctness and feasibility of the theory is verified by experiment. The proposed method is simple, reliable, and easy to achieve.

---

\* Key Lab of Power Electronics for Energy Conservation and Motor Drive of Hebei Province, Yanshan University, Qinhuangdao 066004, China (lzg@ysu.edu.cn)

\*\* Department of Mechatronics Engineering, Kyungsung University, Busan 608-736, Korea (197239066@qq.com , jwahn@ks.ac.kr)

Received 08 February 2013; Accepted 20 February 2013

## 2. Analyze the system operation of SRG under the rated speed

There are three typically control methods of SRG. They are angle position control (APC), current chopping control (CCC) and voltage chopping control (VCC).

APC method means that the voltage added in the winding on a certain condition, changing winding conduction time through turn-on and turn-off to adjust the phase current, and then control the output power. APC method has some advantages, such as torque adjusting range is large and multiphase can be conducted at the same time. The current peak is mainly limited by rotational electromotive force in APC method. When the speed reduces, the rotational electromotive force decreases which can make the current peak value exceed the current allowable value. So the APC method is not suitable for medium and low speed situation.

VCC method can make up for the deficiency of APC. VCC is the method that make the power switch device work in the pulse width modulation (PWM) mode under the condition that maintain the turn-on and turn-off unchanged. VCC method adjusts average values of the voltage added in winding through adjusting duty ratio of PWM wave to change phase current value.

In view of the merit and demerit of these two kinds of control methods, the system block diagram is shown like Fig.1.

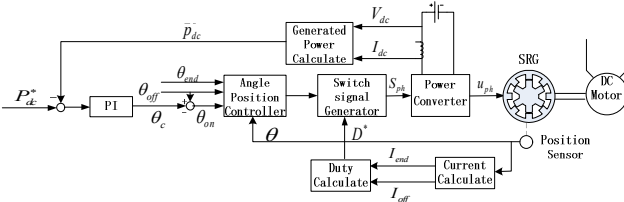


Fig. 1. Block diagram of 8/6-pole SRG system

The block diagram consists of power converter, DC electrical source, controller and position sensor. SRG as the core of the entire system plays a part that absorbs the mechanical energy from the original motivation and delivers the electrical energy to the power source. Voltage equations of each phase are described as follows.

$$u_{ph} = Ri_{ph} + L(i_{ph}, \theta) \frac{di_{ph}}{dt} + \frac{\partial L(i_{ph}, \theta)}{\partial \theta} i_{ph} \omega_r \quad (1)$$

where subscript  $ph$  is one of these phases, the phase inductance  $L$  is the function of the rotor position  $\theta$  and the phase current  $i_{ph}$ , and  $e_{ph} = (\partial L / \partial \theta) i_{ph} \omega_r$  is rotational electromotive force.

In the generator mode, each phase is excited after overlap of stator and rotor poles, where  $(\partial L / \partial \theta) < 0$ , as a result

$$e_{ph} < 0.$$

### 2.1 Power converter and Average output power

Fig. 2 shows the power converter for 8/6-pole SRG, in which  $R$  is load resistance, full bridge rectifier with diodes and filter capacitor  $C$  form a circuit to hold-on DC-link voltage when SRG generates electricity.

When phase resistance is ignored, the derivative of the phase current can be achieved from (1)

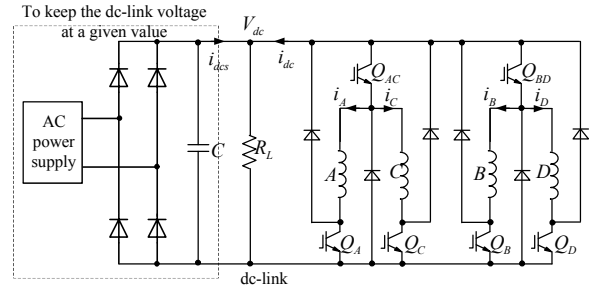


Fig. 2. Power converter with a 8/6 four-phase SRG

$$\frac{di_{ph}}{dt} = \frac{1}{L} (-e_{ph} + u_{ph}) \quad (2)$$

where the phase voltage depends on the state of the switch tubes on each bridge legs, including  $V_{dc}, 0, -V_{dc}$  corresponding to three stages in up and down bridge legs.

The  $u_{ph}$  decides energy transfer direction between SRG and DC source when the phase current was excited. In addition, the change of phase current depends on  $u_{ph}$  and DC-link voltage as in (2). When the operation of the SRG is under the rated speed,  $u_{ph}$  is smaller than  $V_{dc}$ , current can be adjusted by DC-link voltage chopping control when the operation is above the rated speed,  $u_{ph}$  is bigger than  $V_{dc}$ , and phase current is out of control during generation period.

Electric power fluctuates periodically as inherent characteristic in SRG, the period is  $T = \theta_r / \omega_r$  to turn stroke angle. Hence, controlled object should be average power in power control as follows.

$$\overline{P_{dc}} = \frac{1}{T} \int_0^T V_{dc} i_{dc} dt = \frac{V_{dc}}{\theta_r} \int_{\theta_{on}}^{\theta_{on} + \theta_r} i_{dc} d\theta \quad (3)$$

where,  $\theta_r = 2\pi / (mN_r)$ ,  $m$  and  $N_r$  is the number of phases and poles respectively.

### 2.2 Modified APC Method

Fig.3 is the concept waveform of modified APC method. Where,  $L_a$  and  $L_u$  is aligned and unaligned inductance, respectively;  $\theta_{on}$  and  $\theta_{off}$  is turn-on and turn-off, respectively;  $\theta_{fnh}$  and  $\theta_{end}$  is the rotor position at

which phase current extinguishes and stator and rotor pole corners complete overlap, respectively;  $V_{dc}$  and  $i_{ph}$  is the DC-link voltage and phase current, respectively;  $i_{off}$  and  $i_{end}$  is the phase current at  $\theta_{off}$  and  $\theta_{end}$  position, respectively;  $\lambda_{ph}$  is the phase flux linkage. During generator stage, as shown in Fig. 1,  $\theta_{off}$  and  $\theta_{end}$  are constant and the  $\theta_{on}$  is variable. The rotor position and duty ratio can be used to change the state of the switch tubes and then the value of the voltage added on the winding will be altered. The duty ratio can be obtained by  $i_{off}$  and  $i_{end}$ . The value of  $i_{off}$  and  $i_{end}$  can determine the current waveform. The current waveform in the Fig. 3 corresponding to the situation that  $i_{end} > i_{off}$ . So we can obtain the current waveform we needed by using the modified APC method.

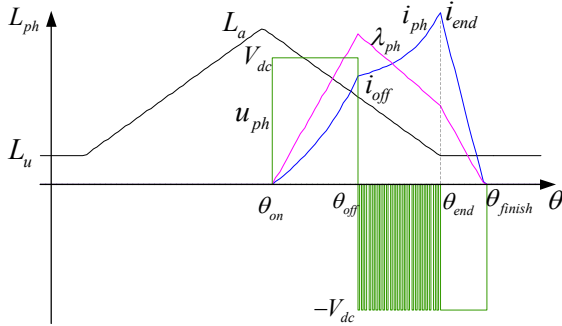


Fig. 3. Concept wave form of modified APC method

### 2.3 The Average Input Mechanical Power and system Efficiency

In the system, the input mechanical power is supplied by DC motor, so the input power can be calculated from (4).

$$P_n = T_e \cdot \Omega = K_T \cdot I_a \cdot \frac{n \cdot \pi}{30} \quad (4)$$

where,  $T_e$  is electromagnetic torque,  $\Omega$  is angle velocity,  $K_T$  is torque coefficient,  $I_a$  is armature current and  $n$  is the motor speed.

From (3) and (4), efficiency is calculated as follows.

$$\eta = \overline{P_{dc}} / P_n \quad (5)$$

### 2.4 Theoretical Analyze of System losses

System losses in the system include copper loss, iron loss, mechanical loss, switching loss and so on, among which the most important are copper loss and core loss. Copper loss depends on phase current rms in (6).

$$p_{cu} = m I_{ph\_rms}^2 s R \quad (6)$$

Phase current rms  $I_{ph\_rms}$  is calculated in (7) by Fig.3.

$$I_{ph\_rms} = \sqrt{\frac{1}{\theta_{rrp}} \int_{\theta_{on}}^{\theta_{fin}} i_{ph}^2 d\theta} \quad (7)$$

where,  $\theta_{rrp} = 2\pi/N_r$  is rotor pole pitch.

Iron loss includes magnetic hysteresis loss and eddy current loss, which is related to the maximum MMF and frequency of alternating magnetic field. Since flux waveforms are non-sinusoidal and flux harmonic spectra differ in various parts of the magnetic circuit, iron loss is not uniformly distributed in the core. An approximate formulae based on Steinmetz equation could be used for iron loss calculation is

$$p_{Fe} = K_h f (B_m)^2 + K_c (f B_m)^2 \quad (8)$$

where  $f$  is the stroke frequency,  $K_h$  and  $K_c$  is the hysteresis and eddy-current loss coefficients, respectively,  $B_m$  is amplitude of flux density for sinusoidal variation.

### 3. Analyze the effect of current waveform on the system efficiency

Fig. 4 is the diagram of the phase current and flux linkage with the various current waveforms at the same output power. Under the rated speed, it can be obtained the three kinds of typical current waveform by adjusting the phase voltage during the power generation stage. They are  $i_{off} < i_{end}$ ,  $i_{off} = i_{end}$ , and  $i_{off} > i_{end}$ . From equation (1), it can be known that the absolute value of phase voltage is smallest when  $i_{off} < i_{end}$ , and the absolute value of phase voltage is biggest when  $i_{off} > i_{end}$ . So at the same output power, the phase current rms is biggest when  $i_{off} < i_{end}$  and as the result, the copper loss is maximum. On the other side, when  $i_{off} > i_{end}$ , the phase current rms is smallest and as the result, the copper

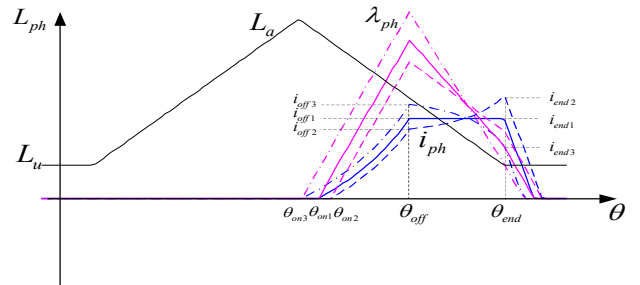


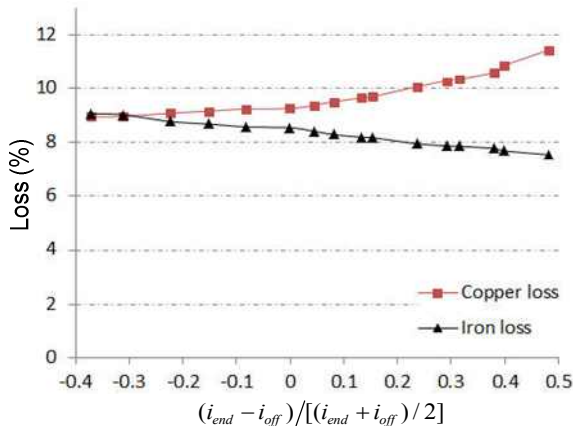
Fig. 4. Phase current and flux linkage with various current Waveform

loss is minimum. In addition, it also can be known from Fig. 4 that the peak value of the flux linkage occurs on the  $\theta_{off}$ . The value is minimum when  $i_{off} < i_{end}$ , and at this time, the core loss is minimum. Inversely, the peak value of flux linkage is maximum when  $i_{off} > i_{end}$ , and at this time, the core loss is maximum.

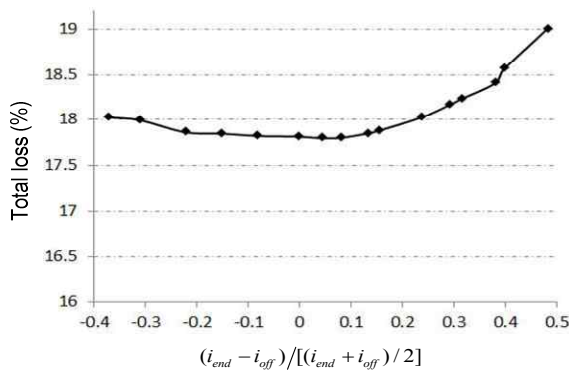
Fig. 5 gives the values of loss with the variation of current waveform at the same output power in the 8/6 four phases SRG system through the Matlab simulation. Fig. 5 (a) is the curve of copper loss and core loss and Fig. 5 (b) is the curve of total loss.

From Fig. 5, it can be known that the copper will increase gradually as the ratio of  $i_{off}$  and  $i_{end}$  from small to large. On the contrary, the core loss will decrease gradually as the ratio of  $i_{off}$  and  $i_{end}$  from small to large. When the  $i_{off}$  approximately equal to the  $i_{end}$ , the total losses is minimum and the efficiency is maximum.

Accurate calculation of the core loss in a motor is essential for computing the actual efficiency. In a SRG, the



(a) copper loss and core loss



(b) total losses

**Fig. 5.** The trend of loss with the variation of current waveform

non-sinusoidal flux waveform with different frequencies of flux reversals in various parts of the motor makes the core

loss calculation difficult. The conventional method for calculation of the core loss is based on the stator pole flux density variation in the triangular fashion with the peak flux density at the rotor position corresponding to the conduction angle from the unaligned position. In this simulation, an accurate method for the calculation of the core loss based on actual flux waveforms in various parts of the SRM is used.

Fig. 6 shows the motor cross section indicating flux density in various parts of the motor. The method used in this simulation is easy to achieve. Because of the flux density of one part shown in Fig. 5, the flux density of other parts can be calculated. The flux density of SP1 and other parts can be calculated by equations (9)~(12).

$$B_{sp1} = \frac{L \cdot i_{ph}}{2 \times N \times A_{sp}} \quad (9)$$

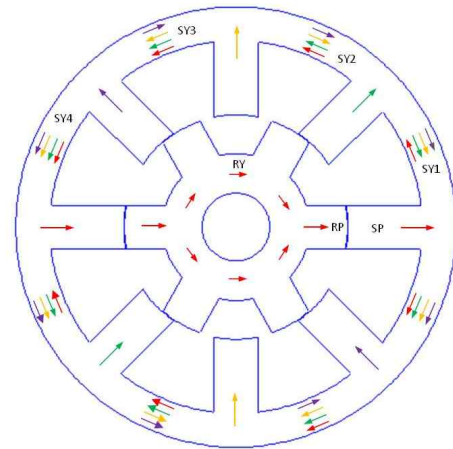


**Fig. 6.** Motor cross section indicating flux density in various parts of the motor

$$B_{rp1} = \frac{A_{sp}}{A_{rp}} B_{sp1} \quad (10)$$

$$B_{sy} = \begin{bmatrix} B_{sy1} \\ B_{sy2} \\ B_{sy3} \\ B_{sy4} \end{bmatrix} = \frac{A_{sp}}{2A_{sy}} \begin{bmatrix} B_{sp1} & -B_{sp2} & -B_{sp3} & -B_{sp4} \\ B_{sp1} & B_{sp2} & -B_{sp3} & -B_{sp4} \\ B_{sp1} & B_{sp2} & B_{sp3} & -B_{sp4} \\ B_{sp1} & B_{sp2} & B_{sp3} & B_{sp4} \end{bmatrix} \begin{bmatrix} 1 \\ 1 \\ 1 \\ 1 \end{bmatrix} \quad (11)$$

$$B_{ry} = \begin{bmatrix} B_{ry1} \\ B_{ry2} \\ B_{ry3} \end{bmatrix} = \frac{A_{rp}}{2A_{ry}} \begin{bmatrix} B_{rp1} & -B_{rp2} & -B_{rp3} \\ B_{rp1} & B_{rp2} & -B_{rp3} \\ B_{rp1} & B_{rp2} & B_{rp3} \end{bmatrix} \begin{bmatrix} 1 \\ 1 \\ 1 \end{bmatrix} \quad (12)$$

where,  $L$  is the phase inductance.  $N$  is the turn number of one pole.  $A_{sp}$ ,  $A_{sy}$ ,  $A_{rp}$ ,  $A_{ry}$  is the area of stator pole, stator yoke, rotor pole and rotor yoke, respectively.

Because the flux density waveform in the SRG is irregular, the FFT method should be used to calculate the maximum and various harmonic components of the flux

density and their corresponding frequencies. The flux density and corresponding frequency which has the important effect on the fundamental flux density are used to calculate the core loss using the equation (8).

### 4. Experimental results and analysis

In order to verify the theory and simulation results of the system efficiency with the various current waveforms, the DC motor and SRG control platform is built. The DC motor as the prime mover and in order to make sure the DC motor can maintain a certain constant speed constant, the DC motor is controlled by speed closed-loop control. The main parameters of SRG are 150V、200W、1500rpm、four-phase and 8/6-pole. In experiment, the TMS320F28335 DSP-150MHz produced by Texas Instruments is used and the cycle for the inner hysteresis current control is 50μs. The frequency of PWM is 20kHz.

power generation stage determined by the difference between  $i_{off}$  and  $i_{end}$ . In addition, the system efficiency is calculated by the output power of DC motor and the generated power of SRG. At this time, with the decrease of the  $\theta_{on}$ , the output power of the SRG will increase, and the phase voltage during the generation stage which maintain the needed current waveform will increase, too.

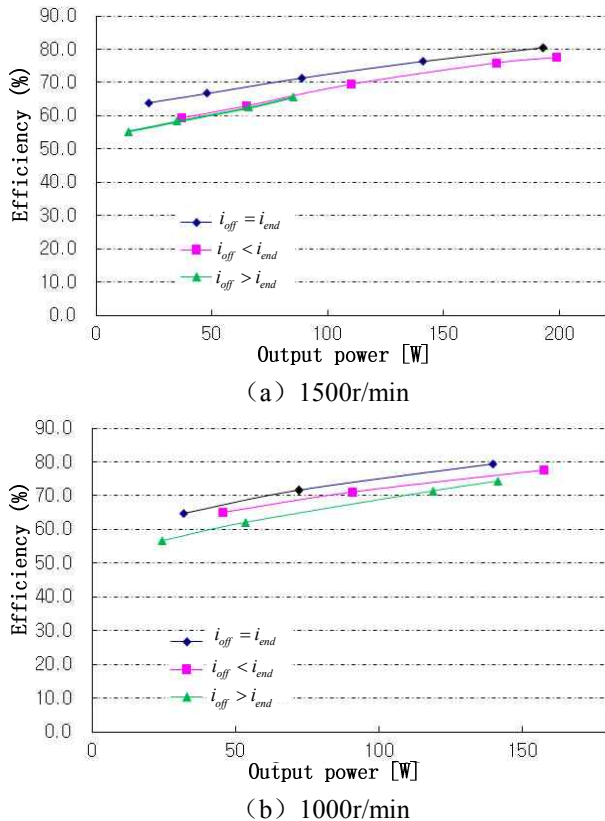


Fig. 7. The trend of efficiency with the variation of output Power

Fig.7 gives the trend of efficiency with the variation of the output power as the speed is 1500rpm and 1000rpm, respectively. In the experiment,  $\theta_{off}$  and  $\theta_{end}$  is fixed at  $41^\circ$  and  $51^\circ$ , respectively and the phase voltage during the

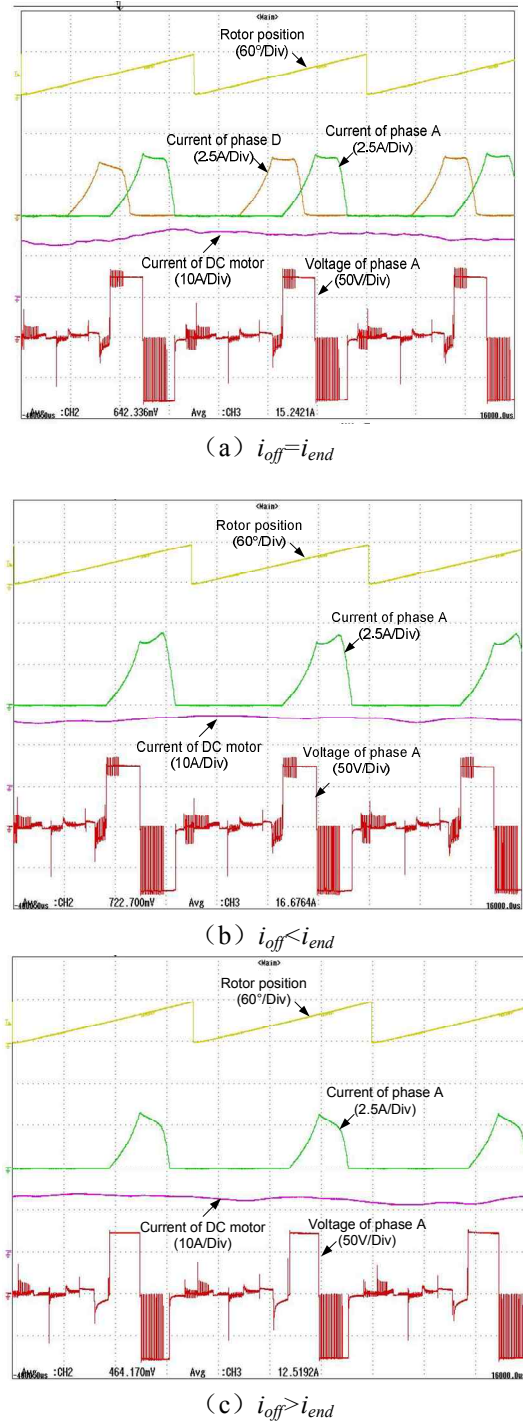


Fig. 8. The experiment waveforms of the three kinds of typical current waveforms

As shown in Fig. 7 (a), when  $i_{off} > i_{end}$ , the reason why the output power less than the rated power is that if the output is continue to increase, the given current shape is not able to maintain. From Fig. 7, it can be seen obviously, when  $i_{off} = i_{end}$ , the system efficiency is maximum at various output power and the results are same with the simulation results.

Fig. 8 gives the position, phase current and phase voltage when running under the three kinds of typical current waveforms.

## 5. Conclusion

In this paper, the high-efficiency operation of SRG in power closed-loop control system is the main objective. The optimum current waveform is obtained by researching the effect of the various current waveforms on the system efficiency. For this purpose, theoretical analysis of the copper loss and iron loss of the system is done first. Then, necessary simulation is done to find the variation trend of the copper loss and iron loss with the variation of the current waveform at the same output power. Finally, the best current waveform which can make the system operate with high efficiency is found by considering the influence of these two kinds of loss. In order to verify the simulation results, the experimental platform of DC motor-SRG is built, and the modified APC method which can specify the current shape optionally is presented. By comparing the system efficiency at the three kinds of typical current waveform, the correctness and feasibility of the theory is verified. The proposed method is simple, reliable and easy to achieve.

## Acknowledgements

This work was supported by the National Research Foundation of Korea(NRF) grant funded by the Korea Government(MEST) (No. 2012-0005022) and by the Natural Sciences Foundation of Hebei Province of China (No. E2010001263).

## References

- [1] T. J. E. "Miller, Electronic Control of Switched Reluctance Machines," Oxford, U.K.: Newnes,Christos Mademlis, Iordanis.
- [2] D. A. Torrey, " Switched reluctance generators and their control," IEEE Trans. Ind. Electron, vol. 49, no. 1, pp. 3-14, Feb. 2002.
- [3] D. E. Cameron and J. H. Lang, "The control of high-speed variable reluctance generators in electric power systems," IEEE Trans. Ind. Appl. , vol. 29, no. 6, pp. 1106-1109, Nov./Dec. 1993.
- [4] Y. Sozer, D. A. Torrey, "Closed loop control of excitation parameters for high speed switched reluctance generators" Power Electronics, IEEE Transactions on, Volume: 19, Issue: 2, March 2004 Pages: 355-362.
- [5] P. Kjaer, P. Nielsen, L. Andersen and F. Blaabjerg, " A new energy optimizing control strategy for switched reluctance motors", IEEE Trans. on Industry Applications, 1995, Vo. 31, No. 5, pp. 1088-1095.
- [6] Kioskeridis, "Optimizing Performance in Current-Controlled Switched Reluctance Generators," IEEE Trans. on energy conversion, Vol.20, No.3, pp.556-565, 2005.
- [7] Iordanis Kioskeridis, Christos Mademlis, "Optimal Efficiency Control of Switched Reluctance Generators," IEEE Trans. on power electronics, Vol.21, No.4, pp.1062-1072, 2006.
- [8] Jawad Faiz, Reza Fazai, "Optimal Excitation Angles of a High Speed Switched Reluctance Generator by Efficiency Maximization," EPE-PEMC 2006, pp.287-291, 2006.



**Zhenguo Li** received the B.S. degree in electric machinery and electrical apparatus from Shenyang University of Technology, Shenyang, China, in 1994, and the M.S. and Ph.D. degrees in mechatronics engineering from Pukyong National University, Busan, Korea, in 2001 and 2005, respectively.

He is currently with Yanshan University, Qinhuangdao, China, as an Associate Professor. His major research field is advanced electrical motor control.



**Siyang Yu** received his B.S. degree in Electrical Engineering from Shenyang University of Technology, Shenyang, China, in 2011. Now he is studying in Kyungshung University, Busan, Korea as a M.S. student in the department of Mechatronics Engineering. His research interests are motor design and

motor control system.



**Jin-Woo Ahn** received his B.S., M.S., and Ph.D. degrees in Electrical Engineering from Pusan National University, Pusan, Korea, in 1984, 1986, and 1992, respectively.

He has been with Kyungsoo University, Busan, Korea, as a professor in the Department of Mechatronics Engineering since 1992. He was a visiting researcher in the Speed Lab at Glasgow University, U.K., a visiting professor in the Dept. of ECE and WEMPEC at the University of Wisconsin-Madison, USA, and a visiting professor in the Dept. of ECE at Virginia Tech from July 2006 to June 2007. He was the director of the Advanced Electric Machinery and Power Electronics Center and President of Korea Regional Innovation System Association. He also has been the director of the Smart Mechatronics Advanced Research and Technology Institute since 2008 and the Senior Easy Life Regional Innovation System since 2008, which are authorized by the Ministry of Knowledge Economy, Korea. He is the author of five books including SRM, the author of more than 150 papers and has more than 20 patents. His current research interests are advanced motor drive systems and electric vehicle drives. He has been the Editor-in-Chief of JICEMS, Chairman of ICEMS2013 and IEEE ICIT 2014.

Dr. Ahn received several awards including the Best Paper Award from the Korean Institute of Electrical Engineers in 2002 and 2011, The Korean Federation of Science and Technology Society in 2003, Korean Institute of Power Electronics in 2007, Park Min-Ho Prize in 2009, Busan Science & Technology Prize in 2011 and Ministerial Citation of Ministry of Knowledge Economy in 2011, ICEMS2012 Outstanding Paper Reward in 2012 respectively. He is a Fellow of the Korean Institute of Electrical Engineers, a member of the Korean Institute of Power Electronics and a senior member of the IEEE.